JOURNAL OF VIROLOGY, May 2008, p. 5031–5042 Vol. 82, No. 10
0022-538X/08/$08.00+0 doi:10.1128/JVI.02069-07

Systemic and Brain Macrophage Infections in Relation to the Development of Simian Immunodeficiency Virus Encephalitis▽

Stephanie J. Bissel,[1]† Guoji Wang,[1] Dafna Bonneh-Barkay,[1] Adam Starkey,[1] Anita M. Trichel,[2] Michael Murphey-Corb,[2] and Clayton A. Wiley[1]*

Departments of Pathology[1] and Molecular Genetics and Biochemistry,[2] School of Medicine, University of Pittsburgh, Pittsburgh, Pennsylvania

Received 18 September 2007/Accepted 27 February 2008

The brains of individuals with lentiviral-associated encephalitis contain an abundance of infected and activated macrophages. It has been hypothesized that encephalitis develops when increased numbers of infected monocytes traffic into the central nervous system (CNS) during the end stages of immunosuppression. The relationships between the infection of brain and systemic macrophages and circulating monocytes and the development of lentiviral encephalitis are unknown. We longitudinally examined the extent of monocyte/macrophage infection in blood and lymph nodes of pigtailed macaques that did or did not develop simian immunodeficiency virus encephalitis (SIVE). Compared to levels in macaques that did not develop SIVE, more ex vivo virus production was detected from monocyte-derived macrophages and nonadherent peripheral blood mononuclear cells (PBMCs) from macaques that did develop SIVE. Prior to death, there was an increase in the number of circulating PBMCs following a rise in cerebrospinal fluid viral load in macaques that did develop SIVE but not in nonencephalitic macaques. At necropsy, macaques with SIVE had more infected macrophages in peripheral organs, with the exception of lymph nodes. T cells and NK cells with cytotoxic potential were more abundant in brains with encephalitis; however, T-cell and NK-cell infiltration in SIVE and human immunodeficiency virus encephalitis was more modest than that observed in classical acute herpes simplex virus encephalitis. These findings support the hypothesis that inherent differences in host systemic and CNS monocyte/macrophage viral production are associated with the development of encephalitis.

Prior to the era of highly active antiretroviral therapy (HAART), approximately 25% of human immunodeficiency virus (HIV)-infected individuals exhibited the pathological hallmarks of HIV encephalitis (HIVE) at autopsy: microglial nodules, multinucleated giant cells, and the presence of abundant activated or HIV-infected macrophages (5, 10, 18, 34, 40). As with other HIV-related sequelae, since the advent of HAART, the incidence of HIVE has decreased (26, 32); however, the prevalence of HIVE has increased, with one report estimating approximately 45% of AIDS autopsies exhibiting HIVE (32). The pathogenesis of simian immunodeficiency virus (SIV)-infected macaque models is remarkably similar to human HIV infection, with a variable percentage of SIV-infected macaques developing SIV encephalitis (SIVE) consisting of similar neuropathology (6, 17, 29, 36, 53). Both of these lentiviral encephalitides show extensive neuronal damage despite an absence of significant neuronal infection (10, 11, 17, 53). Secreted molecules from abundant activated and infected macrophages are thought to interact with neurons or alter supporting glial cell functions to indirectly mediate synaptic damage and subsequent neuronal death (16, 24, 33, 43, 46, 47).

Systemic correlates of lentiviral encephalitis have not been fully identified, and it remains largely unclear why only a fraction of infected individuals develop encephalitis. The incidence and rate of onset (approximately 6 to 36 months after SIV inoculation) vary considerably among different macaque species and with inoculation of different viral strains (6, 17, 67). Virus isolated from the central nervous system (CNS) is macrophage tropic, but inoculation of macaques with macrophage-tropic SIV only is not adequate to induce SIVE (29, 36). Retrospective studies show that macaques that exhibit rapid disease progression (defined as progression to terminal immunosuppression in less than 6 months) are more likely to develop SIVE (62). Even when inoculated with identical viral strains, pigtailed macaques progress to disease more rapidly and have a greater incidence of SIVE than rhesus macaques (35), while cynomolgus and rhesus macaques of Chinese origin rarely exhibit SIV-related neurological sequelae. These observations suggest viral and host factors influence the ability of virus to enter the CNS or replicate in CNS macrophages.

The ability to control SIV replication is thought to influence disease progression rates (20, 25, 51, 52, 55, 57, 61) and possibly development of encephalitis (30, 38, 41, 44, 56). Low anti-SIV antibody titers one month after infection are associated with rapid progression and development of SIVE in pigtailed macaques (44). In the cerebrospinal fluid (CSF) or brain parenchyma of macaques with diffuse neurological symptoms, SIV-specific antibodies or antibody-secreting cells are not de-

* Corresponding author. Mailing address: Department of Pathology, University of Pittsburgh Medical Center, 200 Lothrop Street, A506, Pittsburgh, PA 15213. Phone: (412) 647-0765. Fax: (412) 647-5602. E-mail: claytonwiley@comcast.net.

† Present address: Department of Microbiology, Immunology, and Molecular Genetics, University of California Los Angeles, Los Angeles, CA 90095.

▽ Published ahead of print on 12 March 2008.

TABLE 1. Pigtailed macaque ages, infection parameters, and neuropathological and clinical diagnoses

Monkey no.[a]	Age (mo)	Length of Infection (days)	Diagnosis	
			Neuropathological	Clinical
M156	52	83	Normal	Cough, epistaxis, interstitial pneumonia, enlarged and scrotum and necrotic prepuce
M157	50	137	SIVE, SIV myelitis	Screaming, orchitis, muscle tics
M158	55	185	SIVE, SIV myelitis	Died unexpectedly, SIV hepatitis, SIV enteritis
M159	51	83	SIVE, severe meningitis (gram-positive bacteria)	Died unexpectedly, cytomegalovirus pneumonitis, glomerulosclerosis
M160	52	300	Normal, acute hypoxic changes	Hemorrhagic lung, pneumonitis
M161	59	119	SIVE, SIV myelitis	Ataxia, splenomegaly, severe pneumonia (*Pneumocystis carinii*)

[a] All monkeys were male and had AIDS at the time of sacrifice.

tected (56). Rhesus macaques depleted of $CD8^+$ T cells at the time of infection fail to reduce acute viremia and progress to disease more quickly (51). It has been suggested that these CD8-depleted macaques have an increased incidence of encephalitis (65, 66). The prevalence of $CD8^+$ T cells in the CNS is unclear. Increased numbers of $CD8^+$ T cells correlate with CNS impairment or presence of SIVE in SIV-infected rhesus macaques (30, 38). However, rhesus macaques with *gag*-specific $CD8^+$ T cells in the CSF had minimal CNS infection (41). An increased presence of SIV-specific $CD8^+$ T cells in the CSF was detected in macaques with slow progression and few neurological symptoms (56). These data suggest that the ability of CNS macrophages to produce virus, or the ability of the immune system to control viral replication within and outside the CNS, influences susceptibility to encephalitis.

Because monocytes/macrophages are the predominant infected cells in brains with SIVE and because development of SIVE has been hypothesized to be due to increased trafficking of SIV-infected monocytes (12, 31), we proposed to determine whether monocytes/macrophages from macaques that develop SIVE harbor more replication-competent virus than macaques that do not develop SIVE. Our previous studies suggested that endogenously infected monocyte-derived macrophages (MDMs) from rhesus macaques depleted of $CD8^+$ T cells produced more virus than depleted macaques that did not develop encephalitis. Paradoxically, fewer productively infected macrophages were observed in peripheral organs of macaques with SIVE (9). Here, we show that MDMs from SIV-infected pigtailed macaques that develop SIVE also produce more virus ex vivo, contain more productively infected macrophages in peripheral organs (except for lymph nodes), and have greater numbers of activated T cells in the CNS. These findings support the hypothesis that inherent differences in host control of monocyte/macrophage viral production are related to development of encephalitis.

MATERIALS AND METHODS

Animals. Pigtailed macaques (*Macaca nemestrina*) were housed and maintained according to the standards of the American Association of Laboratory Animal Care and the Institutional Animal Care and Use Committee of the University of Pittsburgh. Macaque information is described in Table 1. Six pigtailed macaques were inoculated with an SIVDeltaB670 viral swarm by intravenous injection at day 0. Macaques were observed daily for clinical signs of anorexia, weight loss, lethargy, or diarrhea. Macaques were euthanized upon development of AIDS-like clinical symptoms. The ages of the macaques ranged from 50 to 59 months (age at time of necropsy). The length of infection varied from 83 to 300 days (median, 128 days). Complete necropsies were performed after humane sacrifice. For Fig. 4, an additional cohort of seven pigtailed macaques was monitored in a similar fashion.

Cell counts. Whole peripheral blood samples (100 μl) obtained from SIV-infected macaques at 0, 7, 14, 21, and 28 days postinfection and every 2 weeks thereafter were stained with fluorochrome-conjugated monoclonal antibodies against CD4 (clone L200; BD Biosciences Pharmingen, San Diego, CA), CD3 (clone FN18; Biosource, Camarillo, CA), and CD8 (clone DK25; DakoCytomation, Carpinteria, CA) for 30 min at 4°C. Red blood cells were lysed using 2 ml Vitalyse (BioE, Inc., St. Paul, MN) for 30 min at room temperature. Cell suspensions were centrifuged and washed with phosphate-buffered saline (PBS) containing 4% fetal bovine serum. Cell suspensions were centrifuged again and resuspended in PBS containing 1% paraformaldehyde. The percentages of $CD8^+/CD3^+$ and $CD4^+/CD3^+$ cells were determined on an XL2 flow cytometer (Beckman Coulter, Hialeah, FL) within 24 h of staining. T cells were gated by CD3 fluorescence and side scatter log. At least 10,000 events were analyzed, and the percentages of $CD4^+$ and $CD8^+$ T cells were determined within the gate. Compensation was done by singly stained peripheral blood mononuclear cells (PBMCs) from each animal. Data analysis was performed using FlowJo (Tree Star, Inc., Ashland, OR). Absolute cell numbers were calculated using percentages of cells and differential cell counts from the blood as previously described (39).

Tissue. Blood samples were obtained prior to infection and on postinfection days 7, 14, 21, and 28 and every two weeks thereafter.

CSF draws were attempted every two weeks postinfection. CSF was aliquoted and stored at −80°C.

Lymph node biopsies were performed at 2, 4, 12, and 16 weeks postinfection (and at necropsy) under ketamine anesthesia at inguinal or axillary sites. Lymph nodes were fixed in 10% buffered formalin (Fisher Scientific, Pittsburgh, PA) and were paraffin embedded. Six-micrometer sections were made for histopathological analysis.

Brains were removed immediately after euthanasia, with the exception of monkeys M158 and M159, and were processed for analysis. M158 and M159 died unexpectedly, and their brains were removed upon discovery. Regional samples were cut from the left hemisphere, snap-frozen, and stored at −80°C. The right hemisphere was fixed in 10% buffered formalin. Coronal sections were made, and tissue blocks were paraffin embedded. Six-micrometer sections were made for histopathological analysis.

Portions of liver, lung, small bowel, thymus, spleen, and spinal cord were removed immediately after and processed in parallel to brain sections. Samples of these organs were not available for M159.

Quantitation of SIV RNA in plasma. Virions from 1 ml of plasma were pelleted by centrifugation at 16,000 × *g* or 23,586 × *g* for 1 h. Total RNA was extracted from the virus pellet using Trizol (Life Technologies, Inc.). Real-time reverse transcriptase PCR was performed with 20 μl of each RNA sample as previously described (7). Primers and probes were specific for the SIV U5/long terminal repeat region.

Histology. To assess each macaque brain for the presence of SIVE, paraffin sections of brain tissue containing neocortical gray and white matter, caudate, putamen, hippocampus, occipital cortex, and cerebellum were stained with hematoxylin and eosin. SIVE was empirically defined as the presence of microglial nodules, multinucleated giant cells, and profuse perivascular mononuclear infiltrates. The morphological distribution and abundance of macrophage/microglia and SIV-infected cells were assessed using a monoclonal antibody against mac-

rophage/microglia-associated protein CD68 (clone KP1; DakoCytomation) and a polyclonal antibody against the SIV envelope gp110 (generously provided by Kelly Stefano Cole and Ron Montelaro, University of Pittsburgh, Pittsburgh, PA), respectively. Sections of midfrontal cortex were also stained for amyloid precursor protein (clone 22C11; Chemicon International, Temecula, CA) and beta-amyloid (clone 6F/3D; DakoCytomation) to assess axonal injury.

Ex vivo cultures to assess p27 production. PBMCs were isolated from whole blood by density gradient centrifugation using lymphocyte separation medium (Mediatech, Inc., Herndon, VA). For MDM cultures, 3×10^6 PBMCs were plated in two-well Lab-Tek Permanox chamber slides (Nalge Nunc International, Rochester, NY) in AIM-V media (Invitrogen, Gibco, Carlsbad, CA) supplemented with 20% fetal calf serum (FCS) and 10 ng/ml monocyte colony-stimulating factor (Sigma-Aldrich, St. Louis, MO). On day 4 of culture, cells were washed three times with sterile PBS to remove nonadherent cells and were maintained in AIM-V supplemented with 20% FCS. Complete media changes were performed at 7, 10, and 14 days postincubation. Virus production was measured on day-14 supernatants using an SIV core antigen ELISA kit (Beckman Coulter) according to the manufacturer's recommendations. The MDMs in the chamber slides were washed three times with PBS and fixed with 4% paraformaldehyde. In order to assess the purity and infection of MDM cultures, slides were immunofluorescently stained for macrophages (CD68), SIV envelope protein (SIVgp110), and T cells (CD3) as described for formalin-fixed paraffin-embedded tissue (7). This affirmed that the majority of cells in the culture were MDMs.

For nonadherent cell cultures, 1×10^6 PBMCs were added to 12-well plates in RPMI 1640 with L-glutamine (Invitrogen, Gibco) supplemented with 10% FCS, 40 U/ml recombinant human interleukin-2 (Roche Diagnostics Corporation, Indianapolis, IN), and 5 μg/ml phytohemagglutinin L (Roche Diagnostics Corporation). On day 4, phytohemagglutinin L was removed by washing the cells in RPMI 1640 with L-glutamine supplemented with 10% FCS and 40 U/ml interleukin-2. Complete media changes were performed at 7, 10, and 14 days postincubation. Cells were maintained at a concentration of 1×10^6 cells/ml. Virus production was measured on day-14 culture supernatants using an SIV core antigen ELISA kit (Beckman Coulter) according to the manufacturer's recommendations.

SIV DNA quantitation. Purified monocytes were obtained from the positive fraction of 10^7 PBMCs that were magnetically separated using CD14 Microbeads (human) (Miltenyi Biotec, Bergisch Gladbach, Germany). Purity ranged from 95 to 98%. Monocyte DNA was isolated using a Qiagen DNA blood mini kit (Qiagen, Valencia, CA) and quantified using a NanoDrop ND-1000 spectrophotometer (NanoDrop Technologies, Wilmington, DE).

Quantitation of cell-associated DNA was performed by real-time PCR in a Prism 7700 detector (Applied Biosystems [ABI], Foster City, CA). The PCR was performed in triplicate by adding 3 μl of each sample to a PCR master mix. The primers and probe used were described previously (7, 21). To generate a standard curve, serial dilutions of DNA containing the SIV target region, ranging from 10^1 to 10^6 copies/reaction, were subjected to PCR in triplicate along with experimental samples. SIV DNA copy numbers from unknown experimental samples were calculated from the standard curve. This result was normalized for volume adjustments (number of SIV DNA copies/cell), multiplied by the number of circulating monocytes/ml blood as determined by complete blood count and differential, and reported as the number of SIV DNA copies from $CD14^+$ monocytes/ml blood.

Analysis of SIV proviral load in PBMCs. DNA was extracted from cryopreserved PBMCs using a DNeasy blood and tissue kit (Qiagen). Samples were boiled for 5 min, and 5 μl was added to a 20-μl cocktail containing 1× real-time PCR master mix (Applied Biosystems) and 600 nM of each amplification primer: forward primer (SGAG21), 5′-TCTGCGTCATPTGGTGCATTC-3′; reverse primer (SGAG22), 5′-CACTAGKTGTCTCTGCACTATPTGTTTTG-3′; and 100 nM probe (pSGAG23), 5′-(FAM)-CTTCPTCAGTKTGTTTCACTTTCTC TTCTGCG-(BHQ)-3′. The assembled reactions were then run on an ABI 7900 sequence detection system (Applied Biosystems). The run conditions and analysis were done as described previously (14). The number of cell equivalents for each DNA sample was determined in a separate assay under the same PCR conditions using primers and probes for *ccr5* as described previously (19). The number of SIV proviral copies per number of cells was calculated based on diploid genome equivalents of the *ccr5* gene.

Immunofluorescent histochemistry. For lymph nodes, paraffin sections containing biopsy tissue were stained for macrophage-associated lysosomal marker CD68 or a polyclonal antibody against CD3 (DakoCytomation) and SIV envelope protein SIVgp110. Double-label immunofluorescent detection was performed with fluoroprobe tags as described previously (7) in order to assess the number of SIV-infected T cells and macrophages.

For liver, lung, small bowel, thymus, spleen, and spinal cord, paraffin sections were stained for CD68, SIVgp110, and CD3 in order to assess the number of SIV-infected T cells and macrophages. Triple-label immunofluorescence staining was performed as described previously (7, 60) using Tyramide Signal Amplification (PerkinElmer Life and Analytical Sciences, Boston, MA) for CD68. This was followed by staining for CD3 and SIVgp110.

For brain, paraffin sections containing midfrontal cortex and basal ganglia were stained for CD3 and T-cell intracellular antigen 1 (TIA-1) (clone 2G9A10F5; Beckman Coulter) in order to assess the number of cytolytic effector cells. Double-label immunofluorescent detection was performed with fluoroprobe tags as described for lymph node staining.

Counting of SIV-infected cells in organs and lymph nodes. Regions of interest were analyzed by laser confocal microscopy (LSM 510; Zeiss, Jena, Germany). The illumination was provided by argon (458, 477, 488, and 514 nm; 30 mW) lasers. Each image was scanned along the *z* axis and the middle sectional plane was found (262,144 pixels per plane; 1 pixel, 0.25 μm^2). Digital images were captured and analyzed with LSM 510 3.2 software (Zeiss). Each organ or lymph node from each macaque was randomly scanned by an individual blinded to the status of the macaques in 10 microscopic areas (40×) encompassing 106,100 μm^2. Scanning parameters such as laser power aperture, gain, and photomultiplier tube settings for each wavelength were kept constant for each macaque specimen. Three or four blinded reviewers enumerated the number of double-labeled cells ($CD68^+$ $SIVgp110^+$ or $CD3^+$ $SIVgp110^+$) and single-labeled SIV-positive cells. The three or four values from each observer were averaged to represent the number of infected cells in that organ area.

Counting of $CD3^+$ and TIA-1^+ cells. Slides with sections of midfrontal cortex and basal ganglia were immunofluorescently stained with antibodies to CD3 and TIA-1. Additional cases of SIV-infected pigtailed macaques with and without histological evidence of encephalitis were included (SIVE, $n = 6$; SIV, $n = 6$). For comparison, sections from human cases diagnosed with West Nile virus encephalitis (WNVE) ($n = 4$), herpes simplex virus encephalitis (HSVE) ($n = 1$), HIVE ($n = 6$), and HIV without encephalitis ($n = 4$) were also analyzed. The regions of interest were viewed using an epifluorescence microscope (Nikon). Each brain section from each case was randomly scanned by an individual blinded to the status in 10 microscopic areas (20×) encompassing 212,200 μm^2. Blinded reviewers enumerated the number of double-labeled cells ($CD3^+$ TIA-1^+) and single-labeled cells ($CD3^+$ and TIA-1^+). Values from each observer were averaged to represent the number of cells in the brain.

Statistical analysis. Data were analyzed using either Microsoft Excel or PRISM 4.0b software (GraphPad Software, Inc., San Diego, CA). We compared each separate variable in two independent, unpaired groups using two-tailed Mann-Whitney tests for nonparametric independent comparisons with 95% confidence intervals. Data were analyzed comparing macaques with SIVE to macaques without encephalitis at each time point rather than comparing the longitudinal trend within the same group.

RESULTS

Four of six SIV-infected pigtailed macaques developed encephalitis. Six pigtailed macaques were infected with SIVDeltaB670 and monitored during the course of infection until clinical symptoms required humane sacrifice. Table 1 summarizes clinical and pathological diagnoses for each macaque. Upon histopathological evaluation, four macaques developed SIVE (67%). One macaque that developed SIVE had terminal acute gram-positive bacterial meningitis. Two macaques did not show evidence of SIVE based on immunohistochemical evaluation for CD68-positive macrophages and SIV-infected cells. One macaque without encephalitis showed acute hypoxic changes in the CA1 region of the hippocampus. The average length of infection was 131 days (median, 128 days; range, 83 to 185 days) for macaques with SIVE and 191.5 days (median, 191.5 days; range, 83 to 300 days) for macaques without encephalitis.

Changes in circulating $CD4^+$ and $CD8^+$ T-cell counts during the course of infection. Preinfection average $CD4^+$ and $CD8^+$ T-cell counts were higher in macaques that developed SIVE than in SIV-infected macaques that did not develop SIVE

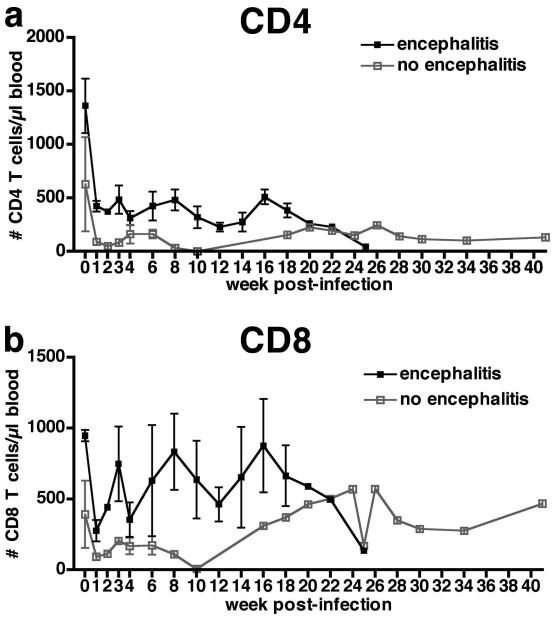

FIG. 1. Mean longitudinal peripheral blood counts for $CD4^+$ and $CD8^+$ T cells of six pigtailed macaques infected with SIVDeltaB670. Based on histological findings, macaques were retrospectively classified at postmortem examination for presence of SIVE. Macaques that developed encephalitis had higher average $CD4^+$ and $CD8^+$ T-cell counts prior to infection and maintained higher average T-cell counts. (a) Mean peripheral blood absolute $CD4^+$ T-cell counts decreased during the first week postinfection (wpi) and remained decreased for the duration of infection. Macaques that developed SIVE (solid black boxes) had greater average $CD4^+$ T-cell counts than macaques without encephalitis (open gray boxes) until 10 wpi. (b) Mean peripheral blood $CD8^+$ T-cell counts decreased during the first wpi and then made a partial recovery before decreasing again. Macaques that developed SIVE (solid black boxes) had greater average $CD8^+$ T-cell counts than macaques without encephalitis (open gray boxes) until 18 wpi.

(Fig. 1) and remained higher until 10 and 18 weeks postinfection for $CD4^+$ and $CD8^+$ T cells, respectively. In this small number of animals, these differences were not statistically significant. The relative loss of $CD4^+$ T cells showed similar trends in both macaques that did and did not develop encephalitis with very few $CD4^+$ T cells present at death (Fig. 1a).

Plasma viremia during the course of infection. During the first 4 weeks of infection, both macaques that did and did not develop encephalitis had high plasma viremia (Fig. 2). Beginning at 6 weeks postinfection, mean plasma viremia was approximately 1 order of magnitude higher in macaques that developed SIVE than in nonencephalitic macaques, but this did not reach statistical significance.

Longitudinal ex vivo virus production from MDMs and nonadherent PBMCs. The ability of infected monocytes to replicate virus was assessed ex vivo. Cultured MDMs were monitored for SIV p27 production at 1, 2, 3, and 4 weeks postinfection and every 2 weeks thereafter when enough blood was available to isolate the cells. The peak p27 production from adherent peripheral blood MDMs of the four macaques that developed encephalitis was an average of 3.6-fold higher than in macaques that did not develop SIVE (21.7 versus 6 ng/ml p27, respectively) (Fig. 3b). The time points postinfection that these differences were observed varied for each macaque (Fig. 3a). All macaques showed higher ex vivo p27 production from MDMs within the first 8 weeks postinfection. M158 showed peak virus production at 16 weeks postinfection. The number of SIV DNA copies associated with $CD14^+$ blood monocytes was also examined at these time points by real-time PCR. Three of the macaques that developed SIVE had numbers of SIV DNA copies in monocytes at 2, 4, or 8 weeks postinfection that were higher than in macaques without SIVE (data not shown).

To investigate this trend further, we were able to monitor the number of infected PBMCs in relation to CSF viral load every 2 weeks postinfection in a separate group of macaques ($n = 7$) (Fig. 4). These animals were sacrificed when moribund with AIDS or, if they survived, at 6 months postinfection. In this cohort, four macaques showed histological evidence of SIVE. This was reflected in the terminal CSF viral load (average, 1.8×10^6 viral copies/ml; range, 1.3×10^5 to 3.7×10^6 viral copies/ml). The remaining three macaques showed no encephalitis. Two of the nonencephalitic macaques had postmortem CSF viral loads less than 10^3 copies/ml, while M280 had 3.4×10^5 viral copies/ml in the CSF despite having no evidence of SIVE. Macaques that developed SIVE had significantly greater numbers of infected PBMCs/mm^3 blood (509 to 10,424 infected PBMCs) at the terminal time points than did macaques that did not develop encephalitis (19 to 53 infected PBMCs). Interestingly, in the weeks prior to death, the elevation of the

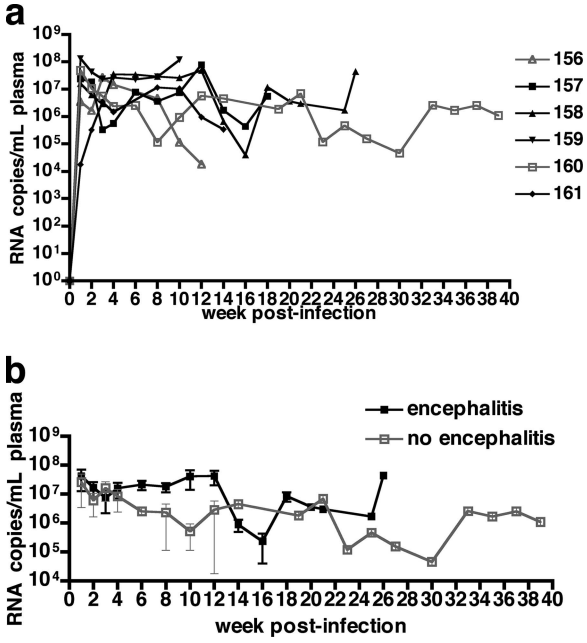

FIG. 2. Plasma SIV RNA of six pigtailed macaques infected with SIVDeltaB670. Based on histological findings, macaques were retrospectively classified at postmortem examination for presence of SIVE. Plasma viral loads in macaques that developed encephalitis were higher from 6 to 12 weeks postinfection (wpi) than for macaques that did not develop encephalitis. (a) Longitudinal plasma SIV RNA levels for the four macaques with SIVE are shown as solid black boxes, and the two macaques without encephalitis are shown as open gray boxes. (b) The mean longitudinal plasma SIV RNA levels for macaques shown in panel a. Plasma viremia was similar for macaques with and without encephalitis during the first 4 wpi. From 6 to 12 wpi, plasma viremia was higher in macaques that developed encephalitis than in macaques that did not develop encephalitis.

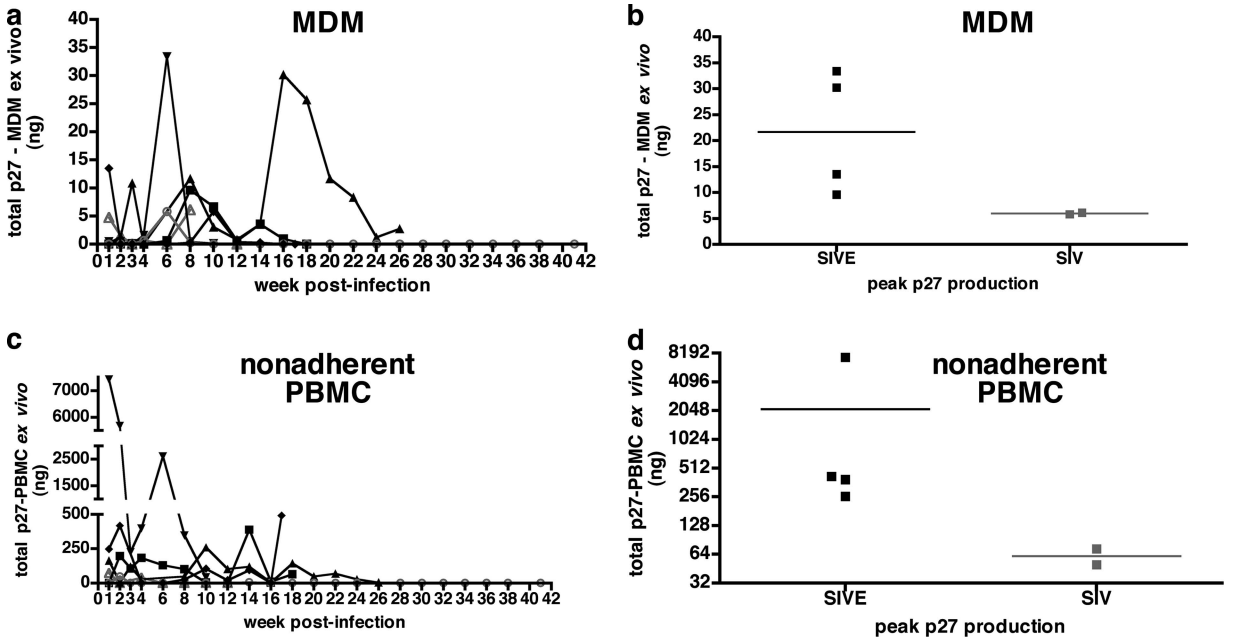

FIG. 3. Longitudinal analysis of SIV p27 production in MDMs and nonadherent PBMCs from six pigtailed macaques infected with SIVDeltaB670. Based on necropsy histological findings, macaques were retrospectively classified for presence of SIVE. (a) At various times during the course of infection, p27 production of MDMs (adherent PBMCs) cultured ex vivo for 14 days showed that the four macaques that developed SIVE (solid black symbols) produced more p27 in culture than the two macaques without encephalitis (open gray symbols). MDMs from each macaque that developed SIVE had peak ex vivo virus production at different times postinfection, mostly within the first 8 weeks postinfection. (b) Peak p27 production from MDMs cultured ex vivo. (c) Longitudinal p27 production levels of nonadherent PBMCs cultured ex vivo for 14 days were increased at various times postinfection from the four macaques that developed SIVE (solid black symbols) compared to the levels in two macaques without encephalitis (open gray symbols). (d) Peak p27 production from nonadherent PBMCs cultured ex vivo.

CSF viral load preceded the rise in the number of infected PBMCs in the encephalitic animals.

Separate nonadherent PBMC cultures from the original cohort of six macaques were also monitored for viral production. Nonadherent cells were capable of producing more virus than adherent MDM cultures, but there were time points where MDM cultures produced more virus than nonadherent PBMC cultures from the same macaque. Peak p27 production from nonadherent PBMCs cultured ex vivo for 14 days was 3.5- to 14.8-fold higher from macaques that developed SIVE than from macaques that did not develop encephalitis (Fig. 3d). As with MDM cultures, the majority of the viral production occurred at earlier time points postinfection, with peak production occurring at various time points.

The numbers of infected cells in lymph nodes from macaques with and without encephalitis are similar. There were few infected cells in the lymph nodes during the course of infection (Fig. 5). The average number of macrophages infected in lymph nodes throughout the course of infection was less than 1 infected macrophage/field, except for M158 at necropsy (average, 4.7 infected macrophages/field). The average number of $CD3^+$/$SIVgp110^+$ cells was 1 to 2 infected cells/field at 2 weeks postinfection and <1 at 4, 12, and 16 weeks postinfection. There was no distinction between the numbers of infected cells observed in lymph nodes in macaques that did and did not develop SIVE.

At necropsy, macaques with SIVE had more productively infected macrophages in liver, lung, small bowel, spleen, thymus, and spinal cord than did macaques without encephalitis. The numbers of productively infected macrophages and T cells in the liver, lung, small bowel, spinal cord, spleen, and thymus were compared for macaques with and without SIVE. Formalin-fixed, paraffin-embedded tissue was fluorescently immunostained for macrophages (CD68), T cells (CD3), and virus (SIVgp110). Four observers enumerated the number of macrophages ($CD68^+$/SIV-positive cells), infected T cells ($CD3^+$/SIV-positive cells), and SIV-infected cells that did not colocalize with either CD68 or CD3 (SIV-positive/$CD3^-$/$CD68^-$ cells). There were very few cells that did not colabel with either CD3 or CD68 in these tissues (Fig. 6). Macrophages were the most common infected cell in lung, small bowel, spinal cord, spleen, and thymus (Fig. 6b to f), while similar numbers of macrophages and T cells were infected in the liver (Fig. 6a). In all organs examined, the median number of productively infected macrophages was statistically significantly higher in macaques with SIVE than in SIV-infected nonencephalitic macaques. The small bowel had the highest number of infected macrophages of all organs examined. The median number of productively infected T cells was statistically significantly higher in the liver and spinal cord of macaques with SIVE than in those of SIV-infected nonencephalitic macaques (Fig. 6a and d), although few infected T cells were observed in the spinal cord.

At necropsy, macaques with SIVE had more CNS T cells with cytolytic potential than did macaques without encephalitis. To examine the local immune response to SIV replication in CNS macrophages, the number of $CD3^+$ T cells expressing TIA-1 was analyzed in midfrontal cortical and basal ganglia regions of the brain. TIA-1 is a cytoplasmic granule-associated protein expressed in cells with cytolytic potential (3). In the brains of ma-

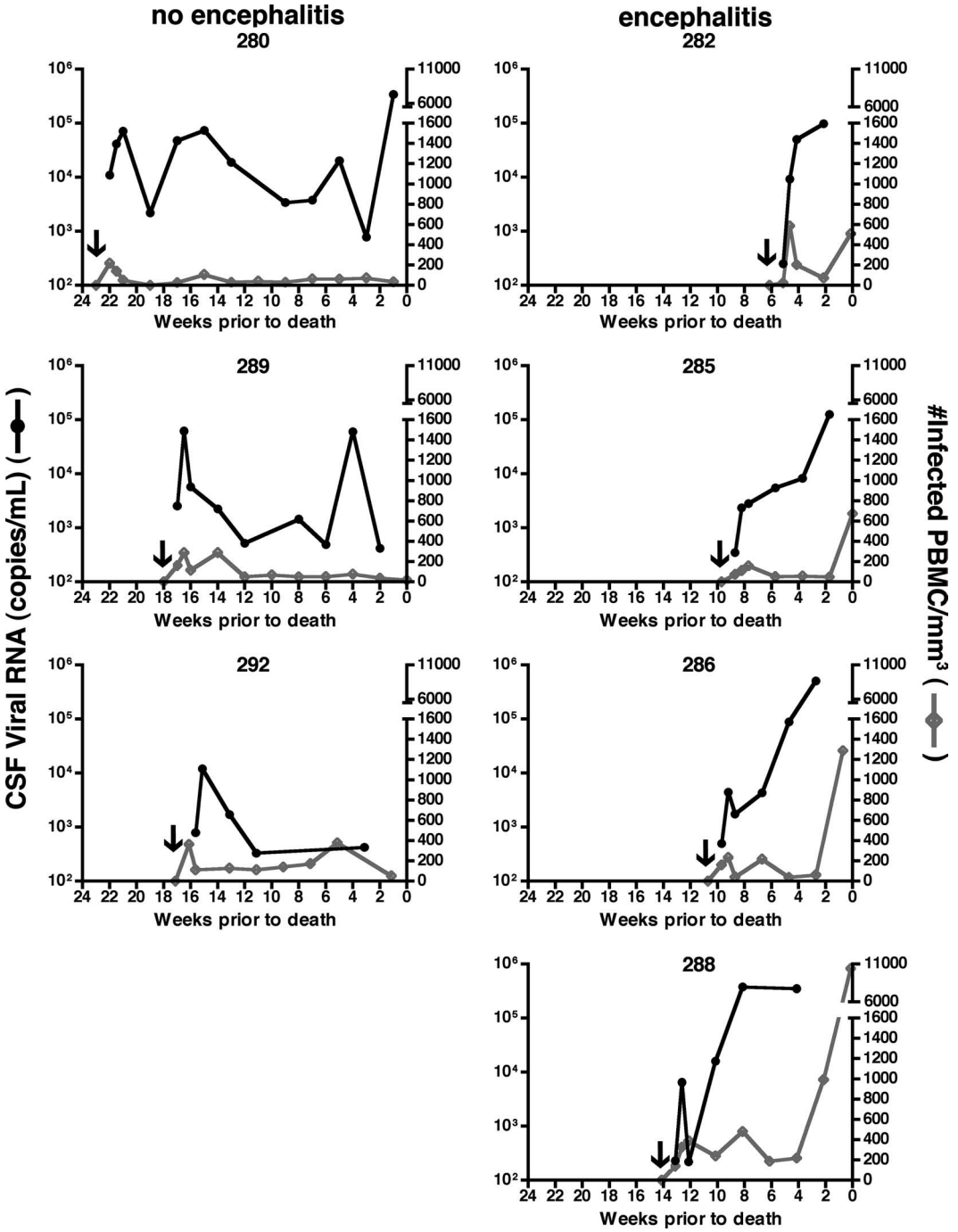

FIG. 4. Longitudinal analysis of CSF viral RNA load and number of infected PBMCs in a cohort of seven pigtailed macaques infected with SIVDeltaB670. Macaques that developed SIVE showed a significant increase in the number of infected PBMCs/mm^3 after an increase in CSF viral load. Macaques were monitored every 2 weeks postinfection. Data are presented as weeks before death because each macaque had a different length of infection. The arrow on each graph indicates when each macaque was infected. The left-hand column shows graphs of individual macaques that did not develop encephalitis (i.e., had no histological evidence of CNS disease), while the right side shows macaques that developed SIVE. The left-hand *y* axis shows the number of CSF viral RNA copies/ml CSF. The right-hand *y* axis shows the number of infected PBMCs/mm^3.

caques with SIVE, there were statistically significantly more CD3$^+$ TIA-1$^+$ cells than in brains of SIV-infected macaques without SIVE (Fig. 7a and c). The numbers of CD3$^+$ TIA-1$^-$ and CD3$^-$ TIA-1$^+$ cells were also greater in brains of macaques with SIVE, but this did not achieve statistical significance. Analysis of brains of patients with HIVE showed a similar trend, but there were fewer CD3$^+$ TIA-1$^+$ cells present in the human disease. Compared to SIVE and HIVE, a human brain with HSVE had a fivefold increase in the number of CD3$^+$ TIA-1$^+$ cells and a greater than 10-fold increase in the number of CD3$^+$ TIA-1$^-$

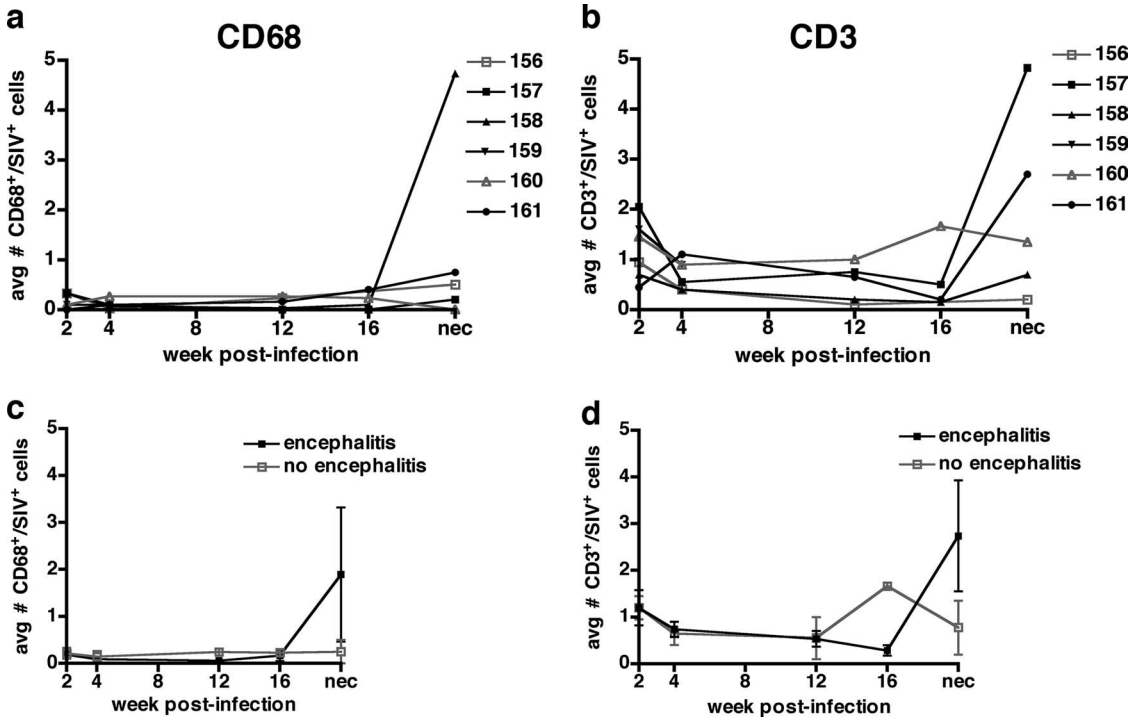

FIG. 5. Longitudinal biopsy survey of the number of infected macrophages and T cells observed in lymph nodes from six pigtailed macaques infected with SIVDeltaB670. Based on histological findings, macaques were retrospectively classified at postmortem examination for presence of SIVE. Each lymph node sample was immunostained for both CD3/SIVgp110 and CD68/SIVgp110 and visualized by immunofluorescent confocal microscopy. Three observers enumerated the number of infected macrophages ($CD68^+$/SIV-positive cells) and infected T cells ($CD3^+$/SIV-positive cells). There were few infected cells in the lymph nodes during the course of infection, and there was no distinction between the numbers of infected cells in lymph nodes from macaques with and without encephalitis. (a) Average number of infected macrophages per microscopic field (106,100 μm^2) for each macaque. Four of five macaques showed slight increases in the number of $CD68^+$/SIV-positive cells at necropsy. Lymph node samples were not available for M159 at 8, 12, and 16 weeks postinfection and at necropsy. (b) Average number of infected T cells per microscopic field (106,100 μm^2) for each macaque. (c) The mean numbers of infected macrophages per microscopic field were similar in macaques with (solid black symbols) and without (open gray symbols) encephalitis. (d) The mean numbers of infected T cells per microscopic field were similar in macaques with (solid black boxes) and without (open gray boxes) encephalitis.

cells. Seventy-five percent and 66% of $CD3^+$ cells colabeled with TIA-1 in the brains of macaques with SIVE and in those of SIV-infected macaques without SIVE, respectively (Fig. 7c and data not shown). Macrophages did not colabel with TIA-1, but TIA-1^+ cells were adjacent to perivascular cuffs of macrophages in the brains of macaques with SIVE.

Macaques with or without SIVE did not have substantial accumulation of amyloid precursor protein or beta-amyloid in midfrontal cortex. Staining for the transmembrane glycoprotein amyloid precursor protein (APP) has been used as an early marker of axonal injury. We stained midfrontal cortical sections from macaques in this study along with archived cases (four additional cases each for SIVE and SIV) for APP and beta-amyloid. Two macaques with SIVE showed modestly stronger somal APP staining of dilated axons in microglial nodules (data not shown). However, there were no substantial focal accumulations of APP in macaques with or without encephalitis. Likewise, beta-amyloid accumulation was not observed in macaques with or without encephalitis (data not shown).

DISCUSSION

Infection of brain macrophages is the predominant feature of lentiviral encephalitis (5, 10, 18, 34, 40). Infected macrophages can be found in the CNS during acute stages of infection (13); however, productively infected CNS cells during the asymptomatic stage of disease are rare (64). Since not all macaques develop encephalitis upon commencement of immunosuppression, the role these early infected macrophages play in the development of encephalitis is not clear. During late stages of immunosuppression, encephalitis is thought to develop when increased numbers of infected monocytes traffic to the CNS (12, 31). It is not known whether macrophage infection is unique to the CNS in animals that develop encephalitis or whether these animals also exhibit abundant blood monocyte and systemic tissue macrophage infection. To begin to determine whether there is an association between systemic and CNS macrophage infections, we analyzed monocyte/macrophage infection during the course of infection in six SIV-infected pigtailed macaques that were retrospectively classified for the presence of SIVE.

Monocyte/macrophage infection during the course of infection. During the course of disease, monocyte viral infections and their capability to produce virus ex vivo were analyzed every 2 weeks. At different time points postinfection, we detected that ex vivo viral production from MDMs from all four macaques that developed SIVE was increased compared to

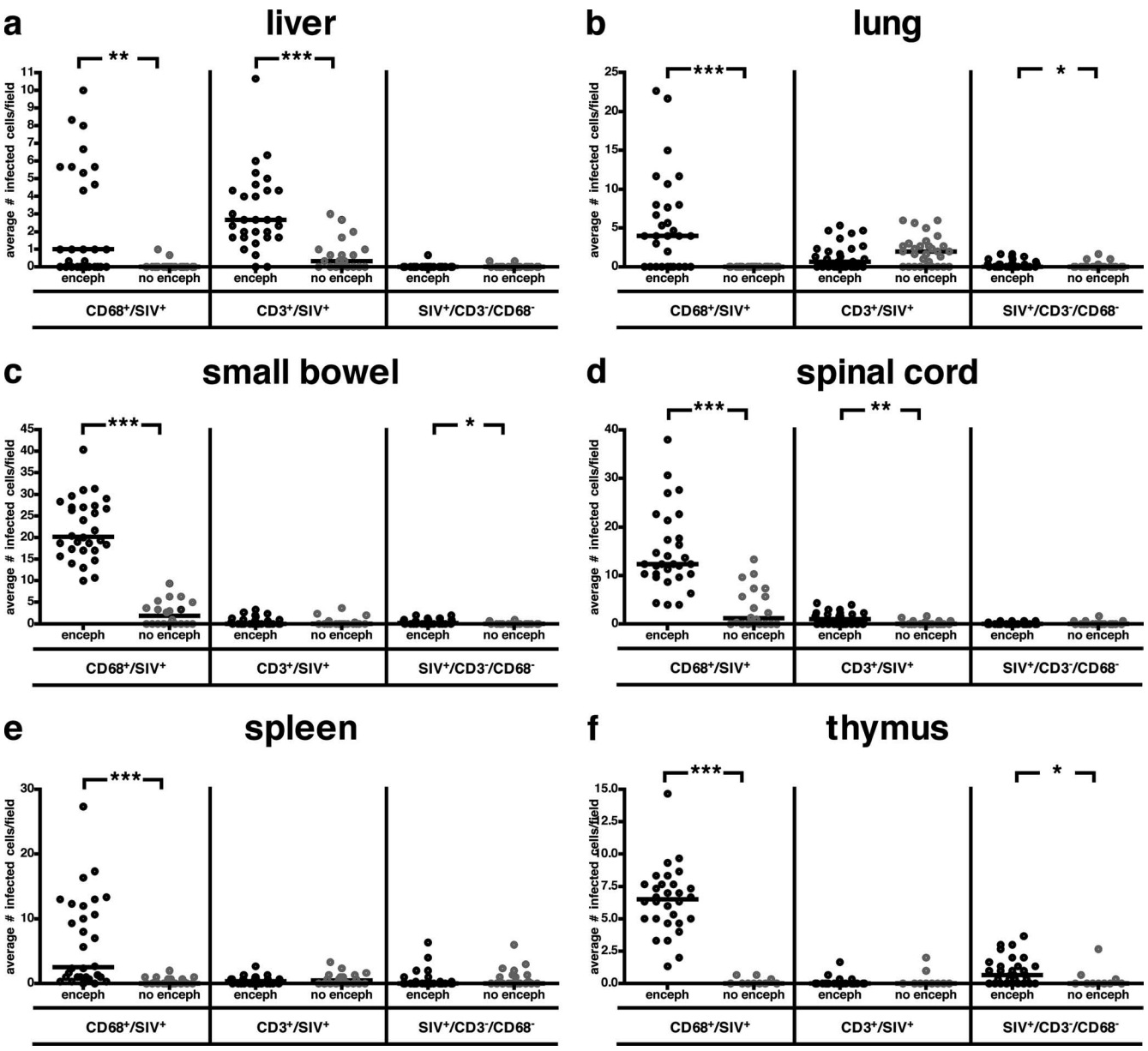

FIG. 6. Pigtailed macaques with SIVE (enceph) have more infected macrophages in peripheral organs than macaques without encephalitis (no enceph). Organs obtained at necropsy were immunostained for CD68, CD3, and SIVgp110 and visualized by immunofluorescent confocal microscopy. Four observers enumerated the numbers of infected macrophages ($CD68^+$/SIV-positive cells), infected T cells ($CD3^+$/SIV-positive cells), and SIV-infected cells that did not colabel with either CD68 or CD3 (SIV-positive/$CD3^-$/$CD68^-$ cells). The black bars represent the median of infected cells enumerated for each group (each dot represents the enumeration from an individual field). (a and d) Liver and spinal cord. The median of infected macrophages was statistically significantly higher in macaques with SIVE than in macaques without encephalitis. More infected T cells were also enumerated in macaques with SIVE than in macaques without encephalitis. Macrophages were the most common SIV-infected cell in the spinal cord. (b, c, and f) Lung, small bowel, and thymus. The median number of infected macrophages was statistically significantly higher in macaques with SIVE than in macaques without encephalitis. Small numbers of SIV-infected cells that did not colabel with CD68 or CD3 were found in the thymus, small bowel, and lung. The small bowel had the highest number of infected macrophages of all organs examined. (e) Spleen. The median number of infected macrophages was statistically significantly higher in macaques with SIVE than in macaques without encephalitis. *, $P < 0.05$; **, $P < 0.01$; ***, $P < 0.001$.

any time point in SIV-infected macaques that did not develop encephalitis. Monocyte-associated viral load was also increased in three of the four macaques that developed SIVE. In order to address how the number of circulating mononuclear cells relates to the development of encephalitis, we isolated PBMCs from an additional cohort of animals and directly assessed the number of infected circulating cells by quantitative reverse transcriptase PCR. A small number of infected PBMCs was detected soon after infection in each macaque regardless of whether they developed encephalitis. However, the macaques that developed encephalitis showed a significant rise in the number of infected circulating cells shortly after

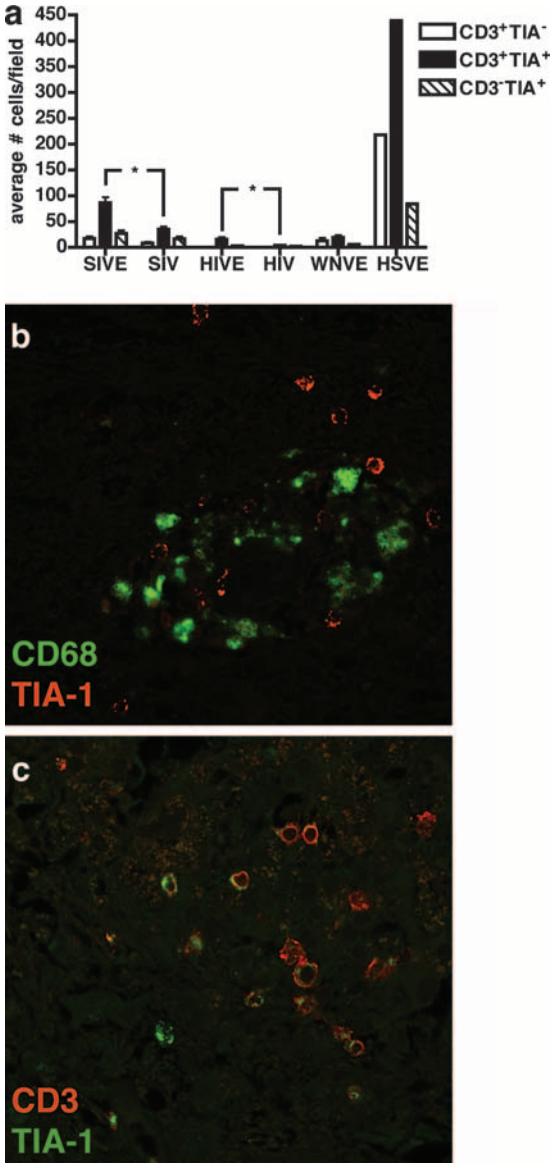

FIG. 7. Pigtailed macaques with SIVE have more $CD3^+$ TIA-1^+ cells in the CNS than macaques without encephalitis. For this analysis, we used banked tissue from six macaques with SIVE and six nonencephalitic SIV-infected macaques. Brain tissue obtained at necropsy was immunostained for TIA-1 and CD3 and visualized by immunofluorescent confocal microscopy. Observers enumerated the numbers of $CD3^+$ TIA-1^- cells, $CD3^+$ TIA-1^+ cells, and $CD3^-$ TIA-1^+ cells. Human brain tissues obtained from autopsies of cases of HSVE, HIVE, HIV infection without encephalitis (HIV), and WNVE were analyzed for comparison. (a) The numbers of $CD3^+$ TIA-1^+ cells were significantly greater in macaques with SIVE than in nonencephalitic SIV-infected macaques. However, the numbers of $CD3^+$ TIA-1^+, $CD3^+$ TIA-1^-, and $CD3^-$ TIA-1^+ cells were more abundant during HSVE than during SIVE and HIVE. *, $P < 0.05$. (b) A perivascular cuff containing macrophages (green, CD68) abutted by TIA-1^+ cells (red) from a macaque with SIVE. (c) Most $CD3^+$ cells in macaques with SIVE are TIA-1^+. Cells were stained for CD3 (red) and TIA-1 (green), with yellow indicating colocalization of CD3 and TIA-1.

developing increased CSF viral load. Therefore, assuming CSF viral load is a correlate of encephalitis (7, 68), the increase in the number of circulating infected cells appears to occur after the development of encephalitis. This suggests that the increased infected CNS macrophages in lentiviral encephalitis are not initiated by newly trafficked cells but are rather due to infection of resident perivascular and parenchymal microglia. Certainly the later spike in circulating infected cells may contribute to the lethal encephalitis.

As with the ex vivo MDM cultures, all four macaques that developed SIVE had nonadherent PBMCs containing $CD4^+$ T cells that produced more virus ex vivo than did the SIV-infected macaques that did not develop SIVE. The highest levels of SIV production were observed during early or mid stages of infection. It is surprising that peak virus production was not seen at the time points immediately before death when the immune response is ablated and the proportion of $CD14^+$ $CD16^+$ blood monocytes is increased as a function of duration of infection (8). However, decreased viral production from nonadherent PBMC cultures was presumably due to the drastic reduction in blood $CD4^+$ T cells during disease progression. Since MDMs produce more virus during earlier stages of infection, rather than prior to death when there are greater numbers of circulating infected cells, it suggests that the ability of cells to produce virus during earlier time points of infection may be more important in the development of encephalitis. Altogether, these data suggest there may be inherent differences in the abilities of individual macaque monocytes and T cells to harbor virus and to produce virus during the course of infection. More apparent, these data show the variability of disease progression and the complexity of the relationship between circulating cells and the development of encephalitis.

Inguinal or axillary lymph node biopsies were performed during the course of infection to analyze the number of infected macrophages. In both macaques that did and did not develop SIVE, there were few infected macrophages present in lymph nodes at the time points analyzed. More surprising was the small number of infected T cells observed at these time points: less than 2 cells/field. High levels of infected cells are generally seen in lymph nodes of rhesus macaques during asymptomatic infection (49). In this study, the pigtailed macaque lymph nodes might have experienced massive replication and cell death prior to the first lymph node biopsy. This would be in agreement with the dramatic decrease in peripheral blood $CD4^+$ T cells seen by the first week after infection. Neither macrophage nor T-cell infection of the lymph nodes correlated with SIVE.

Macrophage infection at necropsy. Pigtailed macaques with SIVE exhibited greater numbers of infected macrophages in all peripheral organs (except lymph nodes) than did macaques without SIVE. The number of infected T cells was also greater in the liver of the macaques with SIVE than in those of SIV-infected nonencephalitic macaques; however, there were few infected T cells in other peripheral organs at necropsy. This may simply reflect severe depletion of $CD4^+$ T cells in tissues at the end stages of disease (45, 50, 58). It is surprising that the number of infected macrophages in the lymph nodes did not mirror the other organs given that the spleen (another secondary lymphoid tissue) showed abundant macrophage infection in macaques with SIVE. Since most lymph nodes were depleted and involuted by necropsy, it is possible that monocytes were migrating to other organs. This suggests that the innate ability of pigtailed macaque macrophages to produce virus in

the CNS and other organs is related to the development of encephalitis.

Such dramatic differences in macrophage infection in peripheral organs were not observed in a group of eight rhesus macaques treated with a $CD8^+$ T-cell-depleting antibody (9). Paradoxically, in this other model, macaques that developed encephalitis had fewer SIV-infected macrophages in the lung and thymus at postmortem than did macaques that did not develop encephalitis. It is possible that rhesus macaques treated with a $CD8^+$ T-cell-depleting antibody have such rapid disease progression that macrophage infection does not have time to develop in every organ. This leaves unexplained why the CNS would be the only organ to show increased macrophage infection in this model.

Immune response to macrophage infection. Few reports have examined immune control of viral infected macrophages in humans or macaques with lentiviral encephalitis (20, 30, 54, 55, 57, 61). Some have identified and described the distribution of $CD8^+$ T cells in association with SIV lesions in the brain (30), and the presence of NK cells has been observed by TIA-1 staining (54). We performed a survey of TIA-1^+ cells in the brain. In macaques with SIVE, the number of T cells ($CD3^+$ TIA-1^+) with cytotoxic potential was significantly higher than in SIV-infected macaques without encephalitis. It is likely that the majority of these cells were $CD8^+$ T cells, since $CD4^+$ T cells are rare in the brains of macaques with SIVE and only a small fraction of $CD4^+$ cells are TIA-1^+. The presence of T cells with cytolytic potential in brains with SIVE indicates that development of SIVE induces an immune response to control CNS viral infection that is not present in the CNS of macaques without SIVE. In the future, it will be necessary to determine whether the local CNS immune response during asymptomatic infection or in animals that do not develop SIVE is sufficient to suppress viral production or whether development of encephalitis is determined by factors outside of the CNS.

The number of T cells with cytolytic potential found in the CNS during HSVE in humans shows that classical acute viral encephalitides induce a much greater local T-cell response than SIV and HIV lentiviral encephalitis and human WNVE. Although HSVE can occur in patients with immunodeficiencies, most patients are immunologically intact, while WNVE, HIVE, and SIVE only occur in immunosuppressed individuals. It would be interesting to determine why the immune responses differ in magnitude in these different encephalitides.

Disrupted axons and beta-amyloid in SIVE. There are numerous descriptions of AIDS patients with and without HIV-related neuropathology as well as pre-AIDS patients showing increased diffuse and focal APP staining compared to controls in subcortical white matter (1, 2, 15, 23, 48, 59, 63). The majority of reports find APP accumulation is not spatially related to HIV-infected foci or prior diagnosis of HIV dementia (23, 48, 63). However, one report found a correlation between APP and HIV p24 staining (42). Similarly, a study found APP staining correlated with SIVgp41 staining and the presence of activated macrophages and microglias and cytotoxic T lymphocytes (37). In this study, we found that some macaques had small foci with moderately stronger somal APP staining, suggesting altered axoplasmic transport limited to microglial nodules, but these small foci were not abundant nor was there substantial APP accumulation. The discrepancies in published reports indicate that a number of factors such as length of infection, age of the patient, prior CNS insults, and length of the presence of lentiviral-infected brain macrophages can contribute to accumulation of APP.

It has also been hypothesized that HIV infection may lead to accelerated brain aging, contributing to neurodegenerative disease and dementia. Beta-amyloid accumulation increases with age and is associated with Alzheimer's disease. Reports conflict on whether there is increased beta-amyloid deposition in HIV-infected patients. Prior to HAART, plaque deposition was not found to increase in AIDS patients compared to levels in age-matched controls (4, 22), except in 3 of 15 young AIDS patients that showed focal perivascular and diffuse beta-amyloid staining (28). After HAART, it has been reported that HAART may increase the presence of perivascular beta-amyloid plaques and neuronal soma and axonal processes (27), while others have seen increased levels of hyperphosphorylated tau- but not premature beta-amyloid deposition (4). We did not observe beta-amyloid staining in the midfrontal cortex in macaques with or without encephalitis. This may be due to the younger ages of the macaques, and premature deposition of beta-amyloid may only occur in older individuals.

In this study we examined the relationship between peripheral SIV infection of monocytes/macrophages and the development of encephalitis. Compared to macaques that did not develop SIVE, the capability of MDMs and nonadherent PBMCs to produce virus ex vivo was increased in macaques that developed SIVE. Prior to death, there was an increase in the number of circulating PBMCs following a rise in CSF viral load in macaques that developed encephalitis but not in nonencephalitic macaques. Macaques with SIVE had more infected macrophages in peripheral organs, with the important exception of lymph nodes. Brains from encephalitic macaques had more T cells with cytotoxic potential than did brains from nonencephalitic macaques; however, there were far fewer activated immune cells in SIVE than in classic acute HSVE. These results suggest that the inherent differences in host viral production by monocytes/macrophages and T cells during the course of infection and macrophages at the end stages of infection are associated with the development of encephalitis. Future studies will determine what host factors account for these inherent differences.

ACKNOWLEDGMENTS

We thank Gokul Kandala, Jonette Werley, and Jessica Garver for valuable technical assistance; Dawn L. McClemens-McBride and Premeela Rajakuman for assistance in obtaining clinical data for the macaques; and Holly Casamassa for valuable veterinary assistance.

This work has been supported by National Institutes of Health (NIH) grants MH071151 and MH01717 to C.A.W. S.J.B. was supported by NIH grant T32MH018273.

REFERENCES

1. **Adle-Biassette, H., F. Chretien, L. Wingertsmann, C. Hery, T. Ereau, F. Scaravilli, M. Tardieu, and F. Gray.** 1999. Neuronal apoptosis does not correlate with dementia in HIV infection but is related to microglial activation and axonal damage. Neuropathol. Appl. Neurobiol. **25:**123–133.
2. **An, S. F., B. Giometto, M. Groves, R. F. Miller, A. A. Beckett, F. Gray, B. Tavolato, and F. Scaravilli.** 1997. Axonal damage revealed by accumulation of beta-APP in HIV-positive individuals without AIDS. J. Neuropathol. Exp. Neurol. **56:**1262–1268.
3. **Anderson, P.** 1995. TIA-1: structural and functional studies on a new class of cytolytic effector molecule. Curr. Top. Microbiol. Immunol. **198:**131–143.
4. **Anthony, I. C., S. N. Ramage, F. W. Carnie, P. Simmonds, and J. E. Bell.**

2006. Accelerated Tau deposition in the brains of individuals infected with human immunodeficiency virus-1 before and after the advent of highly active anti-retroviral therapy. Acta Neuropathol. (Berlin) **111:**529–538.

5. **Bacellar, H., A. Munoz, E. N. Miller, B. A. Cohen, D. Besley, O. A. Selnes, J. T. Becker, and J. C. McArthur.** 1994. Temporal trends in the incidence of HIV-1-related neurologic diseases: multicenter AIDS cohort study, 1985–1992. Neurology **44:**1892–1900.
6. **Baskin, G. B., M. Murphey-Corb, E. D. Roberts, P. J. Didier, and L. N. Martin.** 1992. Correlates of SIV encephalitis in rhesus monkeys. J. Med. Primatol. **21:**59–63.
7. **Bissel, S. J., G. Wang, M. Ghosh, T. A. Reinhart, S. Capuano III, K. Stefano Cole, M. Murphey-Corb, M. J. Piatak, J. D. Lifson, and C. A. Wiley.** 2002. Macrophages relate presynaptic and postsynaptic damage in simian immunodeficiency virus encephalitis. Am. J. Pathol. **160:**927–941.
8. **Bissel, S. J., G. Wang, A. M. Trichel, M. Murphey-Corb, and C. A. Wiley.** 2006. Longitudinal analysis of activation markers on monocyte subsets during the development of simian immunodeficiency virus encephalitis. J. Neuroimmunol. **177:**85–98.
9. **Bissel, S. J., G. Wang, A. M. Trichel, M. Murphey-Corb, and C. A. Wiley.** 2006. Longitudinal analysis of monocyte/macrophage infection in simian immunodeficiency virus-infected, CD8+ T-cell-depleted macaques that develop lentiviral encephalitis. Am. J. Pathol. **168:**1553–1569.
10. **Budka, H.** 1991. Neuropathology of human immunodeficiency virus infection. Brain Pathol. **1:**163–175.
11. **Budka, H., C. A. Wiley, P. Kleihues, J. Artigas, A. K. Asbury, E.-S. Cho, D. R. Cornblath, M. C. Dal Canto, U. DeGirolami, D. Dickson, L. G. Epstein, M. M. Esiri, F. Giangaspero, G. Gosztonyi, F. Gray, J. W. Griffin, D. Henin, Y. Iwasaki, R. S. Janssen, R. T. Johnson, P. L. Lantos, W. D. Lyman, J. C. McArthur, K. Nagashima, N. Peres, C. K. Petito, R. W. Price, R. H. Rhodes, M. Rosenblum, G. Said, F. Scaravilli, L. R. Sharer, and H. V. Vinters.** 1991. HIV-associated disease of the nervous system: review of nomenclature and proposal for neuropathology-based terminology. Brain Pathol. **1:**143–152.
12. **Chakrabarti, L., M. Hurtrel, M. A. Maire, R. Vazeux, D. Dormont, L. Montagnier, and B. Hurtrel.** 1991. Early viral replication in the brain of SIV-infected rhesus monkeys. Am. J. Pathol. **139:**1273–1280.
13. **Clements, J. E., T. Babas, J. L. Mankowski, K. Suryanarayana, M. J. Piatak, P. M. Tarwater, J. D. Lifson, and M. C. Zink.** 2002. The central nervous system as a reservoir for simian immunodeficiency virus (SIV): steady-state levels of SIV DNA in brain from acute through asymptomatic infection. J. Infect. Dis. **186:**905–913.
14. **Cline, A. N., J. W. Bess, M. Piatak, Jr., and J. D. Lifson.** 2005. Highly sensitive SIV plasma viral load assay: practical considerations, realistic performance expectations, and application to reverse engineering of vaccines for AIDS. J. Med. Primatol. **34:**303–312.
15. **Cosenza, M. A., M. L. Zhao, S. L. Shankar, B. Shafit-Zagardo, and S. C. Lee.** 2002. Up-regulation of MAP2e-expressing oligodendrocytes in the white matter of patients with HIV-1 encephalitis. Neuropathol. Appl. Neurobiol. **28:**480–488.
16. **Crowe, S. M.** 1995. Role of macrophages in the pathogenesis of human immunodeficiency virus (HIV) infection. Aust. N. Z. J. Med. **25:**777–783.
17. **Czub, S., J. G. Muller, M. Czub, and H. K. Muller-Hermelink.** 1996. Impact of various simian immunodeficiency virus variants on induction and nature of neuropathology in macaques. Res. Virol. **147:**165–170.
18. **Davies, J., I. P. Everall, S. Weich, J. McLaughlin, F. Scaravilli, and P. L. Lantos.** 1997. HIV-associated brain pathology in the United Kingdom: an epidemiological study. AIDS **11:**1145–1150.
19. **DeGottardi, M. Q., S. K. Lew, M. Piatak, Jr., B. Jia, Y. Feng, S. J. Lee, J. M. Brenchley, D. C. Douek, T. Kodama, J. D. Lifson, and D. T. Evans.** 2008. Comparison of plasma viremia and antibody responses in macaques inoculated with envelope variants of single-cycle simian immunodeficiency virus differing in infectivity and cellular tropism. J. Virol. **82:**321–334.
20. **Dykhuizen, M., J. L. Mitchen, D. C. Montefiori, J. Thomson, L. Acker, H. Lardy, and C. D. Pauza.** 1998. Determinants of disease in the simian immunodeficiency virus-infected rhesus macaque: characterizing animals with low antibody responses and rapid progression. J. Gen. Virol. **79:**2461–2467.
21. **Fuller, D. H., P. A. Rajakumar, L. A. Wilson, A. M. Trichel, J. T. Fuller, T. Shipley, M. S. Wu, K. Weis, C. R. Rinaldo, J. R. Haynes, and M. Murphey-Corb.** 2002. Induction of mucosal protection against primary, heterologous simian immunodeficiency virus by a DNA vaccine. J. Virol. **76:**3309–3317.
22. **Gelman, B. B., and K. Schuenke.** 2004. Brain aging in acquired immunodeficiency syndrome: increased ubiquitin-protein conjugate is correlated with decreased synaptic protein but not amyloid plaque accumulation. J. Neurovirol. **10:**98–108.
23. **Giometto, B., S. F. An, M. Groves, T. Scaravilli, J. F. Geddes, R. Miller, B. Tavolato, A. A. Beckett, and F. Scaravilli.** 1997. Accumulation of beta-amyloid precursor protein in HIV encephalitis: relationship with neuropsychological abnormalities. Ann. Neurol. **42:**34–40.
24. **Giulian, D., J. Yu, X. Li, D. Tom, J. Li, E. Wendt, S. N. Lin, R. Schwarcz, and C. Noonan.** 1996. Study of receptor-mediated neurotoxins released by HIV-1-infected mononuclear phagocytes found in human brain. J. Neurosci. **16:**3139–3153.
25. **Goldstein, S., C. R. Brown, H. Dehghani, J. D. Lifson, and V. M. Hirsch.** 2000. Intrinsic susceptibility of rhesus macaque peripheral $CD4^+$ T cells to simian immunodeficiency virus in vitro is predictive of in vivo viral replication. J. Virol. **74:**9388–9395.
26. **Gray, F., F. Chretien, A. V. Vallat-Decouvelaere, and F. Scaravilli.** 2003. The changing pattern of HIV neuropathology in the HAART era. J. Neuropathol. Exp. Neurol. **62:**429–440.
27. **Green, D. A., E. Masliah, H. V. Vinters, P. Beizai, D. J. Moore, and C. L. Achim.** 2005. Brain deposition of beta-amyloid is a common pathologic feature in HIV positive patients. AIDS **19:**407–411.
28. **Izycka-Swieszewska, E., A. Zoltowska, R. Rzepko, M. Gross, and J. Borowska-Lehman.** 2000. Vasculopathy and amyloid beta reactivity in brains of patients with acquired immune deficiency (AIDS). Folia Neuropathol. **38:**175–182.
29. **Joag, S. V., E. B. Stephens, D. Galbreath, G. W. Zhu, Z. Li, L. Foresman, L. J. Zhao, D. M. Pinson, and O. Narayan.** 1995. Simian immunodeficiency virus SIV_{mac} chimeric virus whose *env* gene was derived from SIV-encephalitic brain is macrophage-tropic but not neurovirulent. J. Virol. **69:**1367–1369.
30. **Kim, W. K., S. Corey, G. Chesney, H. Knight, S. Klumpp, C. Wuthrich, N. Letvin, I. Koralnik, A. Lackner, R. Veasey, and K. Williams.** 2004. Identification of T lymphocytes in simian immunodeficiency virus encephalitis: distribution of CD8+ T cells in association with central nervous system vessels and virus. J. Neurovirol. **10:**315–325.
31. **Lane, J. H., V. G. Sasseville, M. O. Smith, P. Vogel, D. R. Pauley, M. P. Heyes, and A. A. Lackner.** 1996. Neuroinvasion by simian immunodeficiency virus coincides with increased numbers of perivascular macrophages/microglia and intrathecal immune activation. J. Neurovirol. **2:**423–432.
32. **Langford, T. D., S. L. Letendre, G. J. Larrea, and E. Masliah.** 2003. Changing patterns in the neuropathogenesis of HIV during the HAART era. Brain Pathol. **13:**195–210.
33. **Lipton, S. A.** 1992. Requirement for macrophages in neuronal injury induced by HIV envelope protein gp120. Neuroreport **3:**913–915.
34. **Maehlen, J., O. Dunlop, K. Liestol, J. H. Dobloug, A. K. Goplen, and A. Torvik.** 1995. Changing incidence of HIV-induced brain lesions in Oslo, 1983–1994: effects of zidovudine treatment. AIDS **9:**1165–1169.
35. **Mankowski, J. L., J. E. Clements, and M. C. Zink.** 2002. Searching for clues: tracking the pathogenesis of human immunodeficiency virus central nervous system disease by use of an accelerated, consistent simian immunodeficiency virus macaque model. J. Infect. Dis. **186**(Suppl 2)**:**S199–S208.
36. **Mankowski, J. L., M. T. Flaherty, J. P. Spelman, D. A. Hauer, P. J. Didier, A. M. Amedee, M. Murphey-Corb, L. M. Kirstein, A. Munoz, J. E. Clements, and M. C. Zink.** 1997. Pathogenesis of simian immunodeficiency virus encephalitis: viral determinants of neurovirulence. J. Virol. **71:**6055–6060.
37. **Mankowski, J. L., S. E. Queen, P. M. Tarwater, K. J. Fox, and V. H. Perry.** 2002. Accumulation of beta-amyloid precursor protein in axons correlates with CNS expression of SIV gp41. J. Neuropathol. Exp. Neurol. **61:**85–90.
38. **Marcondes, M. C., E. M. Burudi, S. Huitron-Resendiz, M. Sanchez-Alavez, D. Watry, M. Zandonatti, S. J. Henriksen, and H. S. Fox.** 2001. Highly activated CD8(+) T cells in the brain correlate with early central nervous system dysfunction in simian immunodeficiency virus infection. J. Immunol. **167:**5429–5438.
39. **Martin, L. N., M. Murphey-Corb, K. F. Soike, B. Davison-Fairburn, and G. B. Baskin.** 1993. Effects of initiation of 3′-azido,3′-deoxythymidine (zidovudine) treatment at different times after infection of rhesus monkeys with simian immunodeficiency virus. J. Infect. Dis. **168:**825–835.
40. **Masliah, E., R. M. DeTeresa, M. E. Mallory, and L. A. Hansen.** 2000. Changes in pathological findings at autopsy in AIDS cases for the last 15 years. AIDS **14:**69–74.
41. **Moniuszko, M., C. Brown, R. Pal, E. Tryniszewska, W. P. Tsai, V. M. Hirsch, and G. Franchini.** 2003. High frequency of virus-specific $CD8^+$ T cells in the central nervous system of macaques chronically infected with simian immunodeficiency virus SIVmac251. J. Virol. **77:**12346–12351.
42. **Nebuloni, M., A. Pellegrinelli, A. Ferri, S. Bonetto, R. Boldorini, L. Vago, M. P. Grassi, and G. Costanzi.** 2001. Beta amyloid precursor protein and patterns of HIV p24 immunohistochemistry in different brain areas of AIDS patients. AIDS **15:**571–575.
43. **Nottet, H. S., D. R. Bar, H. van Hassel, J. Verhoef, and L. A. Boven.** 1997. Cellular aspects of HIV-1 infection of macrophages leading to neuronal dysfunction in in vitro models for HIV-1 encephalitis. J. Leukoc. Biol. **62:**107–116.
44. **O'Neil, S. P., C. Suwyn, D. C. Anderson, G. Niedziela, J. Bradley, F. J. Novembre, J. G. Herndon, and H. M. McClure.** 2004. Correlation of acute humoral response with brain virus burden and survival time in pig-tailed macaques infected with the neurovirulent simian immunodeficiency virus SIVsmmFGb. Am. J. Pathol. **164:**1157–1172.
45. **Pantaleo, G., C. Graziosi, J. F. Demarest, L. Butini, M. Montroni, C. H. Fox, J. M. Orenstein, D. P. Kotler, and A. S. Fauci.** 1993. HIV infection is active and progressive in lymphoid tissue during the clinically latent stage of disease. Nature **362:**355–358.
46. **Power, C., J. C. McArthur, A. Nath, K. Wehrly, M. Mayne, J. Nishio, T. Langelier, R. T. Johnson, and B. Chesebro.** 1998. Neuronal death induced by

brain-derived human immunodeficiency virus type 1 envelope genes differs between demented and nondemented AIDS patients. J. Virol. **72:**9045–9053.
47. **Pulliam, L., J. A. Clarke, M. S. McGrath, D. Moore, and D. McGuire.** 1996. Monokine products as predictors of AIDS dementia. AIDS **10:**1495–1500.
48. **Raja, F., F. E. Sherriff, C. S. Morris, L. R. Bridges, and M. M. Esiri.** 1997. Cerebral white matter damage in HIV infection demonstrated using beta-amyloid precursor protein immunoreactivity. Acta Neuropathologica **93:**184–189.
49. **Reinhart, T. A., M. J. Rogan, D. Huddleston, D. M. Rausch, L. E. Eiden, and A. T. Haase.** 1997. Simian immunodeficiency virus burden in tissues and cellular compartments during clinical latency and AIDS. J. Infect. Dis. **176:** 1198–1208.
50. **Rosenberg, Y. J., P. M. Zack, B. D. White, S. F. Papermaster, W. R. Elkins, G. A. Eddy, and M. G. Lewis.** 1993. Decline in the CD4+ lymphocyte population in the blood of SIV-infected macaques is not reflected in lymph nodes. AIDS Res. Hum. Retrovir. **9:**639–646.
51. **Schmitz, J. E., M. J. Kuroda, S. Santra, V. G. Sasseville, M. A. Simon, M. A. Lifton, P. Racz, K. Tenner-Racz, M. Dalesandro, B. J. Scallon, J. Ghrayeb, M. A. Forman, D. C. Montefiori, E. P. Rieber, N. L. Letvin, and K. A. Reimann.** 1999. Control of viremia in simian immunodeficiency virus infection by CD8+ lymphocytes. Science **283:**857–860.
52. **Seman, A. L., W. F. Pewen, L. F. Fresh, L. N. Martin, and M. Murphey-Corb.** 2000. The replicative capacity of rhesus macaque peripheral blood mononuclear cells for simian immunodeficiency virus in vitro is predictive of the rate of progression to AIDS in vivo. J. Gen. Virol. **81:**2441–2449.
53. **Sharer, L. R., J. Michaels, C. M. Murphey, F. S. Hu, D. J. Kuebler, L. N. Martin, and G. B. Baskin.** 1991. Serial pathogenesis study of SIV brain infection. J. Med. Primatol. **20:**211–217.
54. **Shieh, T. M., D. L. Carter, R. L. Blosser, J. L. Mankowski, M. C. Zink, and J. E. Clements.** 2001. Functional analyses of natural killer cells in macaques infected with neurovirulent simian immunodeficiency virus. J. Neurovirol. **7:**11–24.
55. **Smith, S. M., B. Holland, C. Russo, P. J. Dailey, P. A. Marx, and R. I. Connor.** 1999. Retrospective analysis of viral load and SIV antibody responses in rhesus macaques infected with pathogenic SIV: predictive value for disease progression. AIDS Res. Hum. Retrovir. **15:**1691–1701.
56. **Sopper, S., U. Sauer, S. Hemm, M. Demuth, J. Muller, C. Stahl-Hennig, G. Hunsmann, V. ter Meulen, and R. Dorries.** 1998. Protective role of the virus-specific immune response for development of severe neurologic signs in simian immunodeficiency virus-infected macaques. J. Virol. **72:**9940–9947.
57. **Staprans, S. I., P. J. Dailey, A. Rosenthal, C. Horton, R. M. Grant, N. Lerche, and M. B. Feinberg.** 1999. Simian immunodeficiency virus disease course is predicted by the extent of virus replication during primary infection. J. Virol. **73:**4829–4839.
58. **Veazey, R. S., M. DeMaria, L. V. Chalifoux, D. E. Shvetz, D. R. Pauley, H. L. Knight, M. Rosenzweig, R. P. Johnson, R. C. Desrosiers, and A. A. Lackner.** 1998. Gastrointestinal tract as a major site of CD4+ T cell depletion and viral replication in SIV infection. Science **280:**427–431.
59. **Vehmas, A., J. Lieu, C. A. Pardo, J. C. McArthur, and S. Gartner.** 2004. Amyloid precursor protein expression in circulating monocytes and brain macrophages from patients with HIV-associated cognitive impairment. J. Neuroimmunol. **157:**99–110.
60. **Wang, G., C. L. Achim, R. L. Hamilton, C. A. Wiley, and V. Soontornniyomkij.** 1999. Tyramide signal amplification method in multiple-label immunofluorescence confocal microscopy. Methods **18:**459–464.
61. **Watson, A., J. Ranchalis, B. Travis, J. McClure, W. Sutton, P. R. Johnson, S. L. Hu, and N. L. Haigwood.** 1997. Plasma viremia in macaques infected with simian immunodeficiency virus: plasma viral load early in infection predicts survival. J. Virol. **71:**284–290.
62. **Westmoreland, S. V., E. Halpern, and A. A. Lackner.** 1998. Simian immunodeficiency virus encephalitis in rhesus macaques is associated with rapid disease progression. J. Neurovirol. **4:**260–268.
63. **Wiley, C. A., C. L. Achim, R. Hammond, S. Love, E. Masliah, L. Radhakrishnan, V. Sanders, and G. Wang.** 2000. Damage and repair of DNA in HIV encephalitis. J. Neuropathol. Exp. Neurol. **59:**955–965.
64. **Wiley, C. A., V. Soontornniyomkij, L. Radhakrishnan, E. Masliah, J. Mellors, S. A. Hermann, P. Dailey, and C. L. Achim.** 1998. Distribution of brain HIV load in AIDS. Brain Pathol. **8:**277–284.
65. **Williams, K., X. Alvarez, and A. A. Lackner.** 2001. Central nervous system perivascular cells are immunoregulatory cells that connect the CNS with the peripheral immune system. Glia **36:**156–164.
66. **Williams, K., S. Westmoreland, J. Greco, E. Ratai, M. Lentz, W. K. Kim, R. A. Fuller, J. P. Kim, P. Autissier, P. K. Sehgal, R. F. Schinazi, N. Bischofberger, M. Piatak, J. D. Lifson, E. Masliah, and R. G. Gonzalez.** 2005. Magnetic resonance spectroscopy reveals that activated monocytes contribute to neuronal injury in SIV neuroAIDS. J. Clin. Investig. **115:**2534–2545.
67. **Zink, M. C., A. M. Amedee, J. L. Mankowski, L. Craig, P. Didier, D. L. Carter, A. Munoz, M. Murphey-Corb, and J. E. Clements.** 1997. Pathogenesis of SIV encephalitis. Selection and replication of neurovirulent SIV. Am. J. Pathol. **151:**793–803.
68. **Zink, M. C., K. Suryanarayana, J. L. Mankowski, A. Shen, M. J. Piatak, J. P. Spelman, D. L. Carter, R. J. Adams, J. D. Lifson, and J. E. Clements.** 1999. High viral load in the cerebrospinal fluid and brain correlates with severity of simian immunodeficiency virus encephalitis. J. Virol. **73:**10480–10488.